This article is a *Plant Cell* Advance Online Publication. The date of its first appearance online is the official date of publication. The article has been edited and the authors have corrected proofs, but minor changes could be made before the final version is published. Posting this version online reduces the time to publication by several weeks.

Exocytosis Precedes and Predicts the Increase in Growth in Oscillating Pollen Tubes [W]

Sylvester T. McKenna,[a] Joseph G. Kunkel,[b] Maurice Bosch,[c] Caleb M. Rounds,[b] Luis Vidali,[d] Lawrence J. Winship,[e] and Peter K. Hepler[b,1]

[a] Department of Biology, Long Island University, Brooklyn, New York 11201
[b] Department of Biology, University of Massachusetts, Amherst, Massachusetts 01003
[c] Institute of Biological, Environmental, and Rural Sciences, Aberystwyth University Plas Gogerddan, Aberystwyth, SY23 3EB, United Kingdom
[d] Department of Biology and Biotechnology, Worcester Polytechnic Institute, Worcester, Massachusetts 01609
[e] School of Natural Science, Hampshire College, Amherst, Massachusetts 01002

We examined exocytosis during oscillatory growth in lily (*Lilium formosanum* and *Lilium longiflorum*) and tobacco (*Nicotiana tabacum*) pollen tubes using three markers: (1) changes in cell wall thickness by Nomarski differential interference contrast (DIC), (2) changes in apical cell wall fluorescence in cells stained with propidium iodide (PI), and (3) changes in apical wall fluorescence in cells expressing tobacco pectin methyl esterase fused to green fluorescent protein (PME-GFP). Using PI fluorescence, we quantified oscillatory changes in the amount of wall material from both lily and tobacco pollen tubes. Measurement of wall thickness by DIC was only possible with lily due to limitations of microscope resolution. PME-GFP, a direct marker for exocytosis, only provides information in tobacco because its expression in lily causes growth inhibition and cell death. We show that exocytosis in pollen tubes oscillates and leads the increase in growth rate; the mean phase difference between exocytosis and growth is –98° ± 3° in lily and –124° ± 4° in tobacco. Statistical analyses reveal that the anticipatory increase in wall material predicts, to a high degree, the rate and extent of the subsequent growth surge. Exocytosis emerges as a prime candidate for the initiation and regulation of oscillatory pollen tube growth.

INTRODUCTION

A unique feature of plant development is the delivery of sperm cells to fertilize the egg through the process of pollen tube growth. The polar growth of this highly elongated cell requires the coordination of many cellular features and functions, such as turgor pressure, ion fluxes, organization, and dynamics of cytoskeletal elements, membrane trafficking, and cell wall formation (Heslop-Harrison, 1987; Steer and Steer, 1989; Mascarenhas, 1993; Holdaway-Clarke and Hepler, 2003; Cole and Fowler, 2006; Campanoni and Blatt, 2007; Chebli and Geitmann, 2007; Krichevsky et al., 2007; Cheung and Wu, 2008). Given the magnitude of the growth process, our attention becomes focused on the synthesis, delivery, and secretion of the new material, which must keep pace with the ever-expanding cell wall (Campanoni and Blatt, 2007; Cheung and Wu, 2008). Not only is a massive amount of wall material needed to support growth, but it is deposited at the extreme apex of the cell, a process also observed in root hairs, fern, and moss protonemata, algal rhizoids, and fungal hyphae. An additional important feature of the pollen tube is that it grows very fast; as a consequence, many of the processes mentioned above, notably vesicular trafficking, are amplified to accommodate the delivery of material needed for the rapidly expanding cell wall (Campanoni and Blatt, 2007; Cheung and Wu, 2008).

During cell elongation, material for the new plasma membrane and cell wall is packaged into vesicles derived from the Golgi apparatus. These vesicles move along actin microfilaments to the apical domain where they undergo exocytosis, fusing with the apical plasma membrane and contributing their contents to the cell wall (Heslop-Harrison, 1987; Steer and Steer, 1989; Lancelle and Hepler, 1992; Cheung and Wu, 2008). Due to the necessity of maintaining the appropriate surface-to-volume ratio, much of the secreted membrane is reclaimed by endocytosis (Picton and Steer, 1983; Moscatelli et al., 2007; Bove et al., 2008; Ketelaar et al., 2008). Endocytotic vesicles may quickly cycle back and revisit the apical plasma membrane, or they may join the reverse fountain streaming pattern and be transported toward the base of the pollen tube (Parton et al., 2001; Bove et al., 2008).

Pectins make up the bulk of the secreted material. The homogalacturonans are synthesized as methyl-esters in the Golgi apparatus (O'Neill et al., 1990; Staehelin and Moore, 1995; Bosch and Hepler, 2005) and are secreted as such (Li et al., 1995; Sterling et al., 2001). The enzyme pectin methyl esterase (PME), which is also secreted (Li et al., 2002; Bosch et al., 2005; Tian et al., 2006), catalyzes the deesterification of the homogalacturonans and exposes carboxyl residues, which are cross-linked by Ca^{2+}, leading to gel formation and a stiffening of the cell wall (Catoire et al., 1998; Bosch et al., 2005; Bosch and

[1] Address correspondence to hepler@bio.umass.edu.
The author responsible for distribution of materials integral to the findings presented in this article in accordance with the policy described in the Instructions for Authors (www.plantcell.org) is: Peter K. Hepler (hepler@bio.umass.edu).
[W] Online version contains Web-only data.
www.plantcell.org/cgi/doi/10.1105/tpc.109.069260

Hepler, 2005). Rhamnogalacturonan II residues, which are covalently incorporated into the homogalacturonan chains, also contribute to cell wall structure through the formation of borate diol-esters (Ishii et al., 1999; O'Neill et al., 2001; O'Neill et al., 2004). The non-cross-linked pectins, which are presumably most abundant at the extreme apex of the cell, render the wall extensible, whereas Ca^{2+} and borate cross-linking, which probably occurs primarily on the flanks of the apical dome, imparts rigidity and prevents the cell from bursting. Pectins thus become multipurpose cell wall components with properties that permit the cell to expand rapidly while still retaining enough strength to prevent cell bursting (Willats et al., 2001; Bosch and Hepler, 2005).

An important feature of pollen tube elongation is that the growth rate oscillates (Pierson et al., 1995, 1996; Geitmann et al., 1996; Feijó et al., 2001; Holdaway-Clarke and Hepler, 2003; Moreno et al., 2007). In lily (*Lilium longiflorum* and *Lilium formosanum*), pollen tube growth rates typically vary continuously from a minimum of 100 nm s^{-1} to >500 nm s^{-1} with a period of 20 to 50 s (Pierson et al., 1996; Cárdenas et al., 2008). Additionally, many of the underlying processes also oscillate with the same period, but usually with a different phase than the growth rate (Holdaway-Clarke and Hepler, 2003; Chebli and Geitmann, 2007; Moreno et al., 2007). Thus, growth emerges as a dynamic steady state process resulting from these myriad interacting factors, each of which is oscillating. Some processes, such as cell wall stress relaxation, accelerate growth, and others, such as Ca^{2+} cross-linking of pectates, slow growth. Although the resulting oscillations may vary in intensity and duration, they are nevertheless constrained within limits due to feedback regulation.

Among the several underlying physiological processes, most attention has been given to the status of intracellular Ca^{2+}. This essential ion (Brewbaker and Kwack, 1963) forms a steep tip-focused gradient at the extreme apex of the tube (Rathore et al., 1991; Miller et al., 1992; Malhó et al., 1994; Pierson et al., 1994; Roy et al., 1999) where it may stimulate exocytosis (Battey et al., 1999; Roy et al., 1999). Further studies have revealed that the Ca^{2+} gradient oscillates in magnitude with the same period as growth rate; however, it follows the increase in growth rate by 10 to 40° (Messerli et al., 2000; Cárdenas et al., 2008). Therefore, it becomes an interesting question whether or not the temporal pattern of exocytosis matches that of Ca^{2+}.

In this study, we address the temporal properties of exocytosis as deduced from changes in amount of wall material and from surface appearance of the enzyme PME. We show that these factors oscillate and that their increase anticipates the increase in growth rate. Detailed statistical analysis further reveals that the anticipatory changes in wall material predict the rate and extent of growth that follows, with remarkable fidelity. Exocytosis emerges as a potential initiator and regulator of growth rate oscillations.

RESULTS

Cell Wall Thickness Oscillates and Leads to the Increase in Growth Rate

In previous studies, changes in the apical cell wall thickness had been reported during pulsatile growth of *Gasteria verrucosa* pollen tubes (Plyushch et al., 1995). We have explored this phenomenon in more detail during oscillatory growth of lily pollen tubes. Prior electron microscopy studies indicate that the wall is significantly thicker at the extreme apex than along the flanks of the apical dome (Lancelle and Hepler, 1992). Realizing that the dimensions of the cell wall will be small, we attempted to optimize the optical system for maximum resolution. We used differential interference contrast (DIC), first with a ×40 oil immersion objective lens (numerical aperture [NA] = 1.3) and a dry condenser (NA = 0.85) and subsequently with a ×60 oil immersion objective lens (NA = 1.4), together with an oil immersion condenser (NA = 1.4). The latter configuration was particularly efficacious because of its higher magnification and resolution, which allowed us to satisfy the Nyquist sampling criterion for our CCD camera and resolve the finest detail possible.

Time-lapse images of lily pollen tubes taken at 1- to 3-s intervals reveal in many instances that the apical cell wall changes in thickness during oscillatory growth (Figures 1A and 1B; see Supplemental Movie 1 online). The changes in thickness appear as a separation of dark/light fringes in the DIC images that are dependent on changes in refractive index of the biological material. Specifically, the outer fringe derives from the gradient in refractive index between the medium and the cell wall, while the inner fringe results from the gradient in refractive index between the cell wall and the protoplast (Figure 1A). During growth, we observed that the distance between these two optical fringes oscillates in a pattern that relates to the oscillation in growth rate (Figure 2).

These two optical fringes are usually quite different in magnitude, with the inner fringe normally dominating (Figure 1B). Because of this inequality, the larger fringe masks some portion of the true peak of the smaller fringe. To solve this problem, we first collected line scans of pixel intensity along the midline of the cell through the tip for each DIC image frame in a sequence. Using a custom R script, we then fit the pixel values to a model of two overlapping Gaussian distributions, deriving the best estimate of the location of the inner and outer DIC fringe and the distance between them at each time point (Figure 1B) (see Methods; see Supplemental Data Sets 1 and 2 online).

The data indicate that cell wall thickness, measured as the distance between the inner and outer DIC fringes, oscillates with the same period as growth rate but not with the same phase (Figure 2). To determine the phase shift, we applied cross-correlation analysis, a procedure that has been used extensively to compute the temporal relationship between variables (for details, see Holdaway-Clarke et al., 1997). In brief, cross-correlation analysis compares the entire records of growth and tip thickness for each experiment, allowing us to determine which phase difference between growth and thickness leads to the best match between the two signals. We can discern leading and following events because growth pulses are not identical in timing or pattern and can be related to corresponding changes in tip thickness. The results show that the apical cell wall in both species of lily pollen tubes becomes thicker in anticipation of an increase in growth rate. In the specific example shown in Figure 2, the increase in thickness precedes the increase in growth rate by –99°. The cell shown in Figure 2 is one example from a population of 10 cells in which the mean period of growth

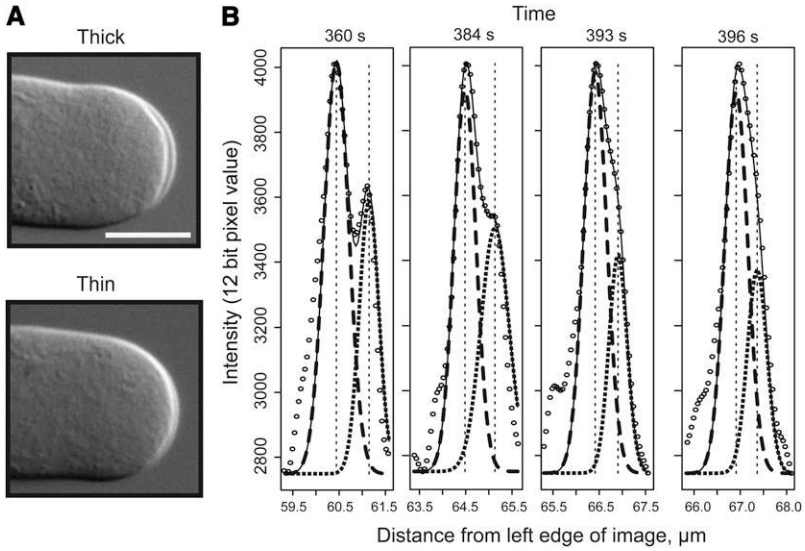

Figure 1. Wall Thickness Changes during Oscillatory Growth in Lily Pollen Tubes.

(A) Two images of the same tube, but at different times, using DIC optics. The top image shows the wall at its thickest state, while the bottom image shows the wall at its thinnest state. DIC generates contrast where there is a sharp gradient in the refractive index. Thus, the two fringes in the top panel correspond to the refractive index gradient between the cell wall and the medium and between the protoplast and cell wall.

(B) A Gaussian fit of the DIC intensity profile, where the origin is the left edge of the image. In this figure, the open circles represent the actual intensity data across the apical cell wall. The large dashed line represents the Gaussian fit for the inner fringe, while the small dashed line the Gaussian fit for the outer fringe. The thin solid line is the sum of the two Gaussian fits. The vertical dashed lines mark the locations of the peaks in each Gaussian fit. Because the intensity of one of the DIC fringes, usually that between the protoplast and cell wall, is normally greater than the other fringe, it masks the information from the minor fringe. This masking is particularly evident when the two fringes come close together as shown in the extreme right graph in **(B)**. For a given pollen tube image, we fit two Gaussian curves to the pixel intensity values of a horizontal line passing through the midpoint of the tip. This allowed us to extract the most likely true positions of the two fringes and measure the distance between them.

oscillation is 24 s $\pm$ 1 s and the phase advance in thickness is 6.6 s $\pm$ 0.4 s or –99° $\pm$ 4.0° (Table 1, first column).

We attempted a similar DIC analysis of tobacco (*Nicotiana tabacum*) pollen tubes, but at no time could we detect a change in the wall thickness. Inspection of electron micrographs, which had been prepared previously using rapid freeze fixation and freeze substitution, reveals that the thickness of the tobacco cell wall at the extreme tip is ~0.25 μm (see Figure 5 in Lancelle and Hepler, 1988), while for lily, it is ~0.5 μm (see Figure 20 in Lancelle and Hepler, 1992). The tobacco cell wall thickness is thus at or below the limit of resolution in our microscopy system, explaining why we have not been able to see changes therein. By contrast, the lily cell wall is thick enough so that changes therein can be resolved at the light microscope level.

Initially we tabulated the phase differences between growth and either wall thickness or propidium iodide (PI) fluorescence (next section) in seconds. We soon realized that the phase advance of both thickness and PI fluorescence correlated with the period of oscillation. As shown in a scatterplot of oscillation periods versus phase differences in lily pollen tubes (Figure 3), including both thickness and PI fluorescence data, the correlation is very robust (R^2 = 0.988). As the oscillation period becomes greater, so too does the advance of wall thickness or PI fluorescence. Therefore, the appropriate fundamental measurement of the relationship between growth and wall property signals is the fraction of a single oscillatory cycle, not the absolute difference in seconds. Our analysis of these phase differences uses methods standard in the signal and time series analysis literature, where a single cycle, like a sine wave, is 360° (Shumway and Stoffer, 2006; Cryer and Chan, 2008). Even though the signals from growth rate and underlying processes are not simple sine waves, we have adopted the standard convention of expressing these fractional phase differences in degrees, which allows us to rigorously compare results from pollen tubes with different average growth rates.

PI Staining Provides a Sensitive Assay for Wall Material in Both Lily and Tobacco

The direct measurement of wall thickness provides evidence for oscillation in the amount of wall material; however, it is restricted due to the resolution limit of the optical system and cannot be applied to tobacco pollen tubes. We know from inspection of electron micrographs that the tobacco cell wall, like that of lily, is thicker at the apex than it is along the flanks of the dome; therefore, we suspect that it also exhibits changes in thickness. To overcome the resolution problem, we used PI, a water-soluble, membrane-impermeant phenanthridium fluorescent dye, to stain the cell wall material. When applied to living plant cells, including pollen tubes (Tian et al., 2006), PI stains cell walls brightly, absorbing over a wide band in the blue and green and emitting in the red (Fiers et al., 2005; Estevez et al., 2008) and

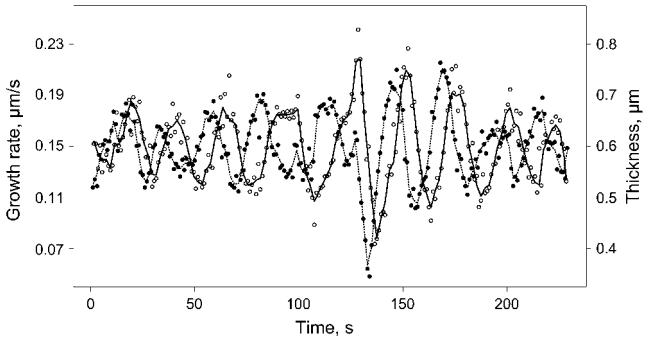

Figure 2. Both Growth Rate and Wall Thickness Oscillate with the Same Period (26 s) but Out of Phase.

Growth rate, acquired from images taken at 1-s intervals, is shown as a solid line (open circles), while the wall thickness is shown as a dotted line (closed circles). Cross-correlation analysis of the data from this cell reveals unambiguously that the increase in thickness precedes the increase in growth rate by 6.9 s or –99°.

localizes in regions known to be pectin rich. Although the basis for staining is not known, PI carries positive charges and may interact with the negative charges that are present on the pectins, especially the carboxyl residues. The basis for PI staining may therefore be similar to other reagents better known for their ability to react with pectin, such as ruthenium red (Ischebeck et al., 2008; Szumlanski and Nielsen, 2009), coriphosphine O (Weis et al., 1988), and nickel or cobalt (Varner and Taylor, 1989; Jauneau et al., 1997), which also carry positive charges. We have applied PI to growing pollen tubes of lily and tobacco. It robustly stains the cell wall of both species without affecting cytoplasmic streaming or the morphology of the tube as observed by DIC; however, there is a slight reduction (5 to 10%) in the growth rate. Fluorescence microscopy reveals staining of the entire cell wall, with the highest level at the apex of both lily and tobacco pollen tubes where the cell wall is thickest (Figures 4A and 4B; see Supplemental Movies 2 and 3 online). This observation is consistent with our interpretation that PI fluorescence serves as a marker for the amount of cell wall material.

Examination of the fluorescence from PI reveals that the level in the apical cell wall oscillates during oscillatory growth in both lily and tobacco pollen tubes (Figures 4A to 4C). Cross-correlation analysis indicates that the fluorescence in a defined region at the extreme apex of the tube increases in anticipation of an increase in growth rate. The advance is –97° ± 4° in lily ($n = 13$; range –74° to –130°) and –124° ± 3.6° ($n = 4$; range –120° to –136°) in tobacco (Table 1). Although the exocytotic advance is not exactly the same between these two species, the agreement is quite close, especially when consideration is given to the evolutionary separation between lily, a monocot, and tobacco, a dicot. Also, in nature, lily pollen tubes grow in a hollow style, whereas tobacco tubes growth through a solid style. Finally, in culture, lily pollen tubes typically grow 5 to 10 times faster than tobacco; moreover, they oscillate much more quickly (29 s versus 67 s).

To further support the claim that PI fluorescence and cell wall thickness monitor the same event, namely, the amount of material in the cell wall, we directly compared these two procedures on the same lily pollen tube. As shown in Figure 4C, the results reveal a very close coincidence between the wall thickness peaks and the PI fluorescence peaks. A quantitative assessment of the same tubes in which the increase in thickness preceded the increase in growth rate by –101° shows that the increase in apical PI fluorescence precedes growth rate by –104°.

To demonstrate that the DIC and PI fluorescence images are monitoring the cell wall and that they are not due to some artifact or optical anomaly, we purposely plasmolyzed the cells and compared the signal from these two procedures on the same pollen tube. When treated with 12% mannitol in all cases ($n = 20$), the cell stopped growing but momentarily continued to secrete wall material, which continued as long as the plasma membrane was in contact with the cell wall. Within a few minutes, though, the protoplast retracted from the apical cell wall. Direct inspection, as shown in Figure 4D, reveals that the DIC and PI fluorescence images superimpose on one another. In particular, the much thickened apical wall appears evident by both microscopy methods, further supporting the idea that PI fluorescence indicates the amount of cell wall material.

Table 1. Phase Difference between Exocytosis and Growth in Lily and Tobacco Pollen

Species		Lily			Tobacco	
Comparison		Thk. versus Growth	PI versus Growth	PI and Thk. versus Growth	PI versus Growth	PME versus Growth
	n	10	13	23	4	4
Period (s)	Range	20 to 31	20 to 49	20 to 49	44 to 96	130 to 142
	Mean	24	33	29	67	136
	SE	1.0	2.7	1.8	11	3
Phase difference (s)	Range	−5 to −9	−6 to −12	−5 to −12	−17 to −32	−35 to −59
	Mean	−6.6	−8.8	−7.9	−23	−49
	SE	0.40	0.60	0.45	3.2	5.3
Phase difference (°)	Range	−75 to −115	−74 to −130	−74 to −130	−120 to −136	−97 to −152
	Mean	−99	−97	−98	−124	−128
	SE	4.0	4.0	3.0	3.6	12

Thk, thickness of apical wall; PI, propidium iodide staining; PME, GFP-tagged pectin methyl esterase fluorescence.

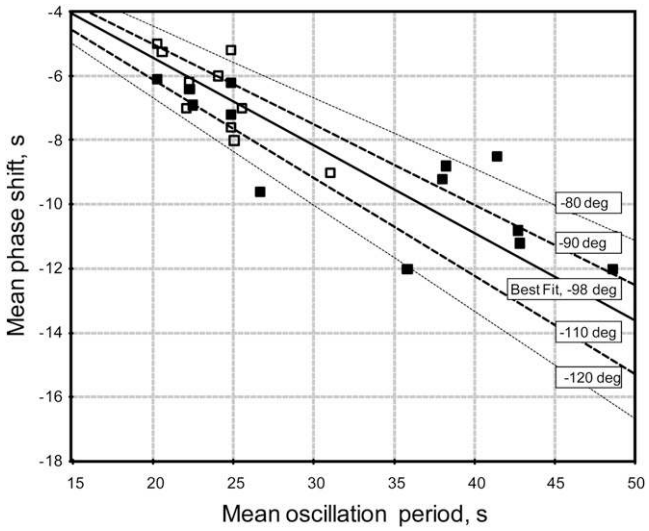

Figure 3. A Scatterplot Shows the Relationship between Oscillation Periods and Phase Differences in Tip Thickness and PI Fluorescence in Lily Pollen Tubes.

Open squares are phase differences for thickness, and closed squares are for PI fluorescence. The central solid line is the least squares best fit (R^2 = 0.988, n = 23) for all data and has a slope equivalent to a phase difference of –98°. The lines above and below the regression line illustrate the phase difference envelopes for the values shown. Note that most phase differences, whether determined by thickness or by PI, fall between –80° and –120°.

Secretion of PME-GFP in Tobacco Pollen Tubes Oscillates and Leads Growth

The above data indicate that the product of secretion, namely, the amount of cell wall material, goes through periodic net increases during oscillatory growth. However, we wanted to test the process of exocytosis more directly, and to that end employed PME (*N. tabacum* PPME1) linked to green fluorescent protein (PME-GFP). We previously reported on the identification and functional characterization of a *N. tabacum* pollen-specific PME, PPME1, showing that this full-length construct contained a preregion and a proregion together with the enzymatic PME domain (Bosch et al., 2005). We further showed that overexpression of PPME1 had no detrimental effect on pollen tube growth. Of particular interest, PME-GFP labeled the secretory pathway and appeared to be secreted to the cell surface (Bosch et al., 2005). The intracellular labeling is consistent with this chimerical protein being localized in the endoplasmic reticulum and the Golgi apparatus. Curiously, PME-GFP, as previously shown by Bosch et al. (2005), does not brightly stain the inverted cone of vesicles in the apical domain. Although there is fluorescence throughout the apical region, the area defined by the inverted cone is usually less bright than the surrounding areas. However, a bright arc of fluorescence appears at the apical cell surface, which fluctuates during growth (Figure 5A; see Supplemental Movie 4 online).

To show more conclusively that the apical surface arc of fluorescence, evident in pollen tubes expressing PME-GFP, represents secretion, we conducted plasmolysis experiments on tobacco pollen tubes expressing this full-length construct. As negative controls, we included pollen tubes expressing partial constructs, which do not exhibit bright arcs at the apical surface and which therefore have been interpreted as not undergoing exocytosis (see Supplemental Figure 1 online). As depicted clearly in Supplemental Figure 1A online, when plasmolyzed, the apical fluorescence of the full-length construct remains with the cell wall, being biased in its distribution with the inner wall layer. The other two constructs (see Supplemental Figures 1B and 1C online), which do not yield bright arcs at the cell apex, also, when plasmolyzed, do not show any fluorescence associated with the cell wall. These data indicate that full-length PME-GFP is secreted.

To provide an indication of the rate and extent of secretion, we measured the fluorescence in a defined region at the apical surface on successive time-lapse images and correlated these with changes in pollen tube growth rate. It is important to note that not all growing tobacco pollen tubes exhibit distinct oscillations in growth rate. In addition, among the tubes expressing PME-GFP, there appeared to be fewer oscillators when compared with control tubes not expressing an introduced fusion protein. Also, the growth rate is reduced by 20%, and the period of oscillation lengthened from 130 to 142 s. Nevertheless, among those tubes expressing PME-GFP, we identified a subset that exhibited clear oscillatory growth. The detailed analysis of these tubes shows that the fluorescence oscillates and that its increase, based on cross-correlation analysis, anticipates the increase in growth rate by –128° ± 12° (n = 4) (Figure 5B, Table 1). Again, we emphasize the close agreement between PI fluorescence and the surface signal of PME; they both anticipate the increase in growth rate by ~120 to 130°. This is true even though the oscillatory period is substantially longer in the cells expressing PME when compared with nonexpressing controls (Table 1).

Although PME-GFP is clearly secreted, the signal is not expressed throughout the thickness of the cell wall nor is it evident along the side walls (see Supplemental Figure 2A online). These observations are in close agreement with the findings of Li et al. (2002) who show with immunogold transmission electron microscopy that PME is only found on the inner layer of the apical cell wall in tobacco pollen tubes and is not distributed throughout the thickness of the wall. Together, these findings suggest that PME-GFP is either degraded or diffuses away relatively quickly. The arc of fluorescence therefore appears to represent only recently secreted material, further supporting the claim that it behaves as a direct marker for exocytosis.

We made an extensive effort to express PME-GFP and other potentially secreted proteins in lily pollen tubes, but without success. Tobacco PME-GFP appears to poison lily pollen tubes, causing much reduced growth and even death. The fluorescence signal in lily tubes is very weak and diffuse, showing no particular localization and no accumulation at the cell surface. Other probes tested included the signal peptide sequence for tobacco extensin and lily polygalacturonase. The last-mentioned probe showed the most promise but even so failed to generate a clear signal that indicated secretion. The problem is under continued investigation because being able to observe secretion in lily would permit us to exploit its marked advantages over tobacco

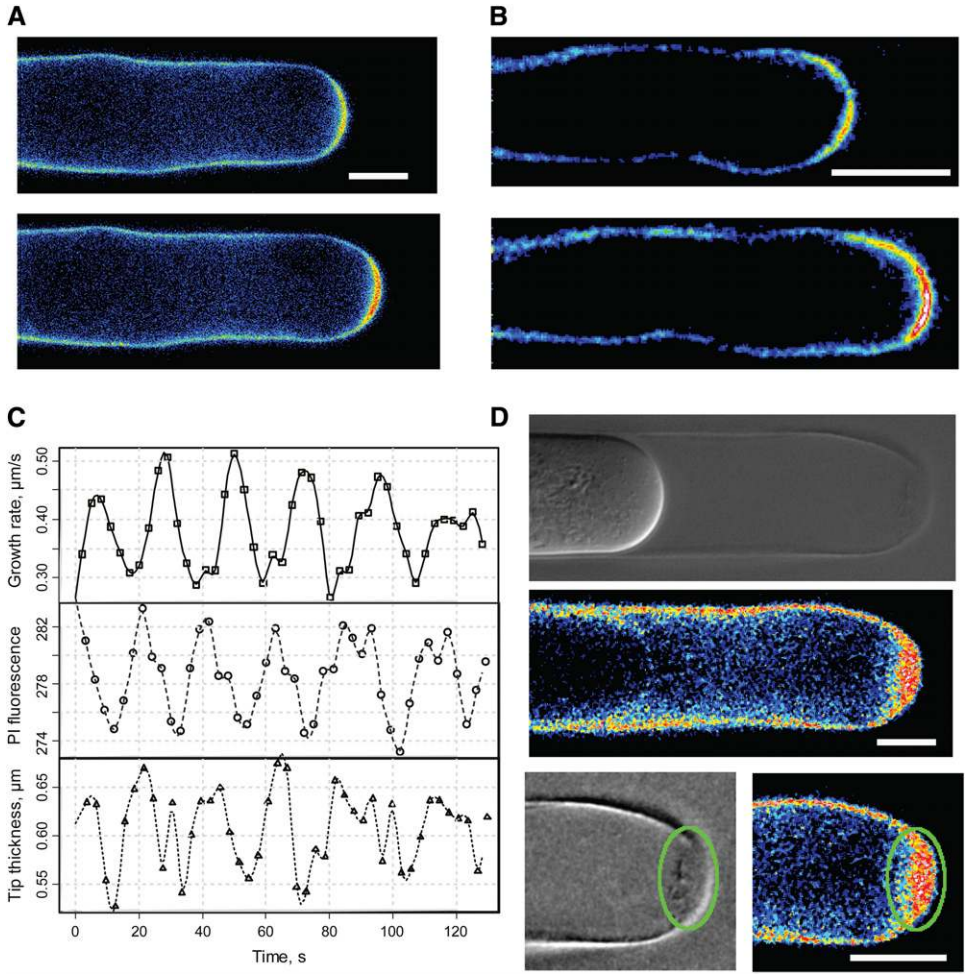

Figure 4. PI Vitally Stains the Cell Wall and Permits Recording of Changes in Wall Material in Both Lily and Tobacco Pollen Tubes.

(A) and **(B)** Lily and tobacco pollen tubes, respectively, with increases in the fluorescence in the bottom panel of each pair compared with the top panel. Also note that fluorescence is strongest at the extreme apex, or growing point, of the cell.

(C) The three graphs depict, from top to bottom, growth rate, PI fluorescence, and wall thickness on the same lily pollen tube. Comparing the bottom two traces reveals that PI fluorescence and thickness provide very similar information. From cross-correlation analysis of this particular experiment, the PI signal leads growth by –104°, while the DIC thickness change leads growth by –101°.

(D) A plasmolyzed lily pollen tube, providing further proof that the externally applied PI selectively stains the cell wall not the protoplast. Comparison of the DIC and fluorescence images indicates that the highest level of PI staining occurs at the extreme apex where the cell wall is thickest (green ovals).

with regard to spatial and temporal resolution of structures and processes.

The Amount of Secreted Wall Material Predicts the Growth Rate

Our studies suggest that the correlation between growth and the amount of wall material is not confined to the frequency of the oscillation but also extends to the magnitude of the growth in each pulse. That is, there appears to be a functional relationship between the amount of wall material at the tip over time and the growth rate that explains much of the pulse-to-pulse variation in peak shape. Visual inspection of growth rate and thickness data plotted on the same axes suggests that a thicker wall precedes a more rapid expansion. Moreover, it is the amount of wall material at a time well before the peak in growth rate that appears to best predict peak growth. To extend this idea, we first conducted a multiple correlation analysis (Maindonald and Braun, 2007) on the data from six pollen tubes. In this analysis, we applied both a general linear model (GLM) and a general additive model (GAM) (Figure 6) in which we used a set of independent variables derived initially from the wall thickness and later from PI fluorescence time series to test how effectively wall properties might predict the growth rate time series. The GLM assumes a linear relationship between the wall thickness and growth rate, while the GAM permits one to use various curvilinear relationships

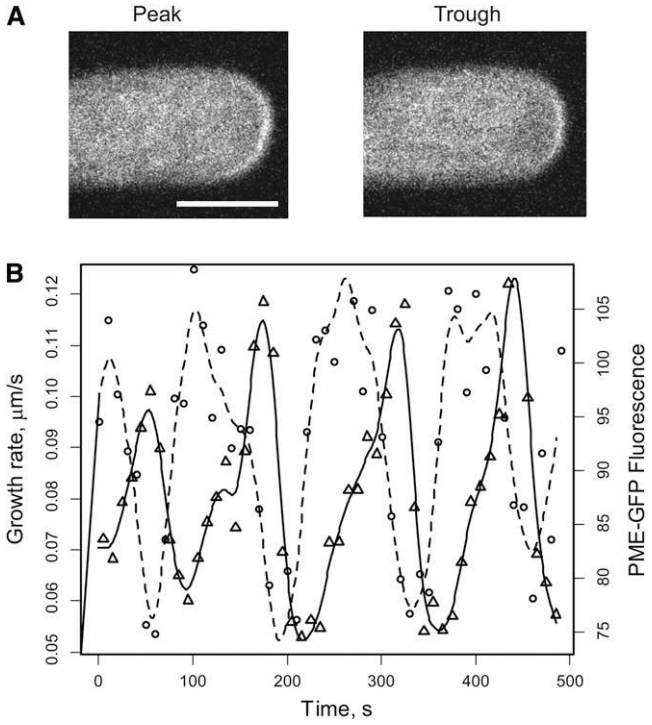

Figure 5. Secretion of PME-GFP Oscillates at the Cell Surface.

(A) The apical region of a tobacco pollen tube expressing PME-GFP. The fluorescent signal at the cell surface oscillates between high (peak; left image) and low (trough; right image) levels.

(B) A trace of growth rate (solid line; triangles) versus changes in PME fluorescence (dashed line; circles). Cross-correlation analysis of a population of four cells reveals that the increase in PME fluorescence at the cell surface leads the increase in growth rate by –128° ± 12°.

when setting up the correlation model, consistent with our supposition that the relationships among the processes regulating tip growth are likely to be nonlinear.

Knowing the phase lag between growth rate and wall thickness, we initially set up an equation in which growth rate, V, at each time point, t, was predicted by a combination of thickness values at times, t', before and after that time point, referred to as offset times. We include terms for individual pollen tubes (j), for the interaction between individual cells and wall thicknesses because we wanted to know how consistent the correlation relationships were from cell to cell:

$$V_t = u + W_{t'} + P_j + PW_{jt'} \quad (1)$$

where u is a grand mean, W is a vector of wall thicknesses at offset times t'. P is the pollen tube effect allowing each tube to have its own additive component. For completeness, we include the possibility that each pollen tube has a unique W, which is represented by a PW or the pollen–tube wall interaction.

The allowable offset times were determined by the times that the DIC images were taken, which was one every 3 s. We considered times before and after the peak in growth rate but within the bounds of surrounding peaks. When the offset time was zero, there was very little predictive value of the wall thickness. However, there were two peaks of predictive power; one for wall thickness prior to peak growth rate and one for wall thickness after the peak growth rate. Using the multivariate test for additional information (Rao, 1965), we were able to ask if a particular time offset or groups of offsets provided any additional information in predicting growth rate. The most powerful predictors were offsets 9 to 21 s prior to peak growth rate and 9 to 21 s after peak growth rate. Wall thickness offsets by −6, −3, 0, 3, and 6 s had no significant ability together or alone in improving the prediction of growth rate. However, the offsets of wall thickness both before and after peak growth rate provided additional pertinent predictive information. For example, offsets of +9 to +21 s significantly improved the prediction of growth rate when used in combination with the −9 to −21 s offsets. That is, in a tip growth cycle, the eventual thinness of the wall can independently combine with the prior preparatory wall thickness to predict a higher rate of expansion.

Figure 6 illustrates the close fit between growth rates predicted by a GLM analysis of the thickness data. A GAM was applied with the reasoning that each width at a given time offset might not be related to growth rate in a simple linear manner. Indeed, the GAM model did give a statistically better fit, 56% (GLM) versus 62% (GAM), but the plotted regression line was not obviously better than the GLM model seen in Figure 6.

The above analysis derives from the summation of six cells and reveals a strong correlation between wall thickness and the subsequent growth rate. The extent of correlation becomes even stronger, even with the more conservative GLM, in analyses of single cells using thickness, but especially PI fluorescence, as a marker for amount of cell wall material (Figures 7A and 7B). It is important to note that there is a greater range in the PI fluorescence data when compared with the wall thickness measurements. For example, the fact that we can derive a signal from tobacco pollen tubes with PI fluorescence, but not from a direct measurement of thickness by DIC, tells us that the fluorescence procedure is the more sensitive one. We predict, therefore, that the statistical correlation between PI fluorescence and growth rate might provide a more meaningful result than between wall thickness and growth rate. Figures 7A and 7B directly compare these two measurements and growth rate in the same lily pollen tube and indicate that the prediction is true. In Figure 7A, the solid line is the best fit of thickness data, the open circles are the growth rate data, and the dotted lines represent the 95% confidence interval of the predicted values. A quantitative analysis indicates that the wall thickness accounts for 71% of the variation in growth rate. An analysis of the PI signal, using similar but not identical offsets on the same cell, indicates that changes in fluorescence account for 79% of the variation in growth rate (Figure 7B).

Finally, we have also examined the correlation between PI fluorescence and growth rate in a single tobacco pollen tube. In Figure 7C, as with those above, the solid line represents the best fit of the PI fluorescence, which has been superimposed on the growth rate data (open circles). Again, the dotted lines represent the 95% confidence interval. In this instance, the quantitative statistical analysis indicates that the change in PI fluorescence accounts for 91% of the variation observed in the growth rate.

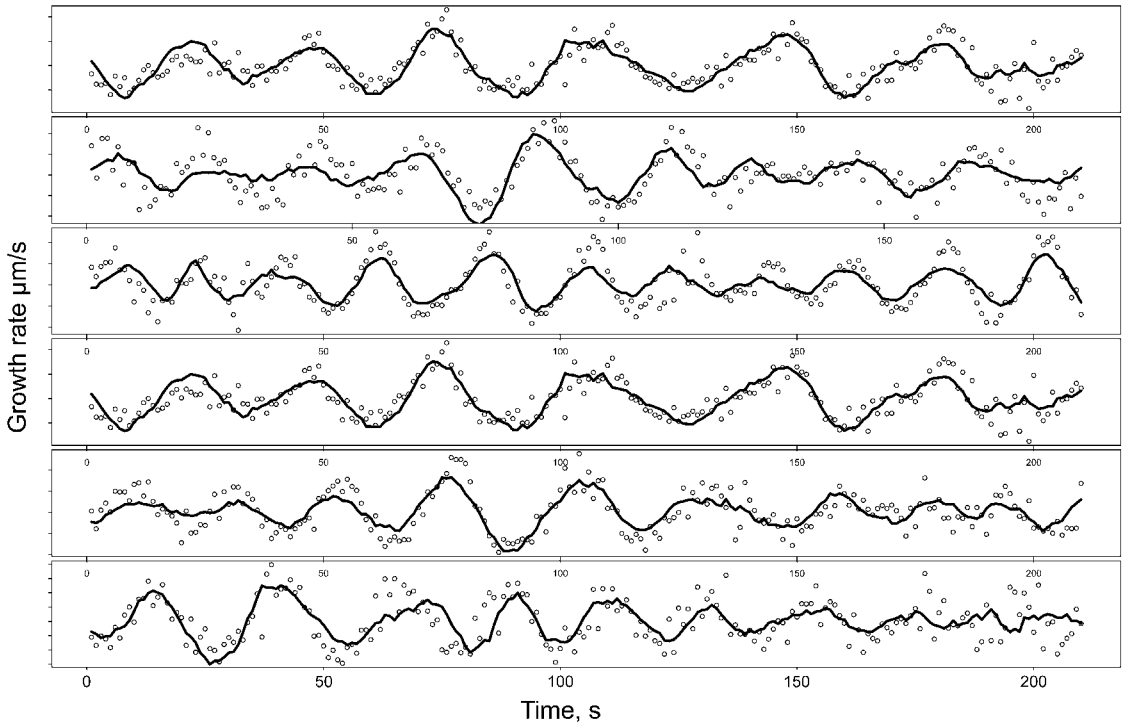

Figure 6. Multiple Correlation Analysis Reveals That the Change in Wall Thickness at the Tip Strongly Predicts the Rate and Extent of Growth.

Six different lily pollen tubes are represented in this graph. The open circles show the growth rate, acquired at 1-s intervals, while the solid line depicts changes in wall thickness. Using either a GLM or a GAM for all six cells, we found that thickness measurements in advance of each growth rate time point combined with measurements after the same time point produced a fit with an R^2 of 0.56 (GLM) and 0.62 (GAM), indicating that cell wall thickness explains ~60% of the variation in growth rate.

DISCUSSION

Exocytosis Oscillates and Leads the Increase in Growth Rate

Our results show that exocytosis, detected by three separate methods, oscillates during pollen tube growth and leads the increase in growth rate. The advance is –98° in lily and –124° in tobacco. Not only is there close agreement between different methods on pollen tubes from the same species, but there is quite good agreement between lily and tobacco. From the observations presented in Results together with the arguments presented below, we feel justified in asserting that exocytosis is a leading event in oscillatory growth and may play a key role as an initiator of cell elongation.

It is first important to establish the basis for the measurements that we have made. Each of the three methods we used relies on different physical principles and each requires some assumptions for interpretation. The most direct method has been to follow the appearance of PME-GFP in the apical cell wall. As a direct marker of exocytosis, it relies on the assumption that once secreted, the PME molecules either move rapidly away from the site of exocytosis and degrade or the GFP tag loses its fluorescence due to quenching by the acid pH in the wall. Under these conditions, the steady state level of PME-GFP in the apoplasm will be dominated by exocytotic addition of new protein. We feel this assumption is warranted since we do not see PME-GFP fluorescence extending out into the wall. In addition, previous work by Li et al. (2002), using immunogold localization of PME, found the enzyme only on the inner layer of the cell wall. From these considerations, we conclude that the changes in PME-GFP fluorescence are directly proportional to the rate of exocytosis.

The other two methods, namely, measurement of wall thickness using DIC optics and wall fluorescence from PI-stained pollen tubes, rely on changes in the amount of wall material.

It is important to emphasize at the outset that because the apical wall is composed almost entirely of pectin and because pectin is processed through the Golgi dictyosomes and delivered to the apoplasm via the secretory pathyway (Nebenführ and Staehelin, 2001), the cell wall is thus the product of exocytosis. However, the material in the cell wall at the cell tip, unlike PME, does not disperse but becomes incorporated into the elongating pollen tube, and the amount represents a balance between exocytosis and local wall expansion. In tobacco, we monitored the amount of wall material by the binding of the fluorescent dye PI to pectin because we were unable to visualize changes in the width of the cell wall with DIC. In lily, we compared PI fluorescence with direct measurement of wall thickness; unfortunately, we were unable to express PME-GFP in lily. Regardless of

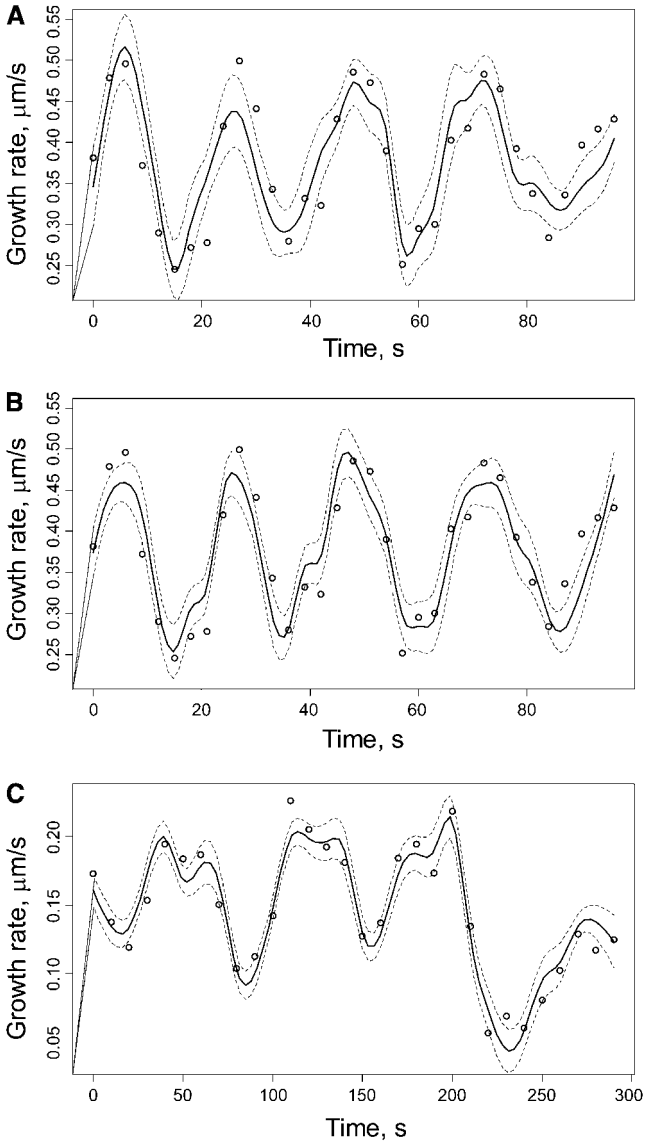

Figure 7. PI Fluorescence Correlates More Strongly with Growth Rate Than Does Wall Thickness.

Note that in each panel the solid line shown is not a smoothed fit to the actual growth data. Rather, it is the growth profile predicted by correlation with thickness or with PI fluorescence values measured at times before and after each time point. Virtually all of the actual growth rate measurements (open circles) fall within the 95% confidence range, shown as dotted lines above and below the multiple correlation line.

(A) A graph showing that growth rate is predicted by tip thickness in a lily pollen tube. Multiple R^2 = 0.7567, adjusted R^2 = 0.7117, and P value = 1.496e^{-07}.

(B) A prediction of the growth rate based on PI fluorescence from the same lily pollen tube shown in **(A)**. Multiple R^2 = 0.8203, adjusted R^2 = 0.7947, and P value = 4.559e^{-10}.

(C) A prediction of the growth rate in a tobacco pollen tube derived from PI fluorescence of the apical cell wall. Multiple R^2 = 0.927, adjusted R^2 = 0.9118, and P value = 7.487e^{-13}.

these differences, which we address in more detail below, we emphasize that there is remarkable agreement among all the methods.

Wall Thickness and PI Fluorescence Are Valid Estimates of the Amount of Wall Material

The measurements both for DIC and PI fluorescence were made along the mid line, or polar axis, of the cell, where new wall material constantly accumulates. Prior electron microscopy analyses of both lily and tobacco pollen tubes indicated that the wall is thickest at the apical midpoint. For live-cell studies, we initially employed DIC, which responds to gradients in refractive index; the two DIC fringes mark the boundaries of the cell wall, with the outer fringe indicating the cell wall/medium interface and the inner fringe the cell wall/cytoplasm interface. PI fluorescence, on the other hand, depends on appropriate binding sites in the wall, with higher fluorescence indicating a greater number of binding sites.

While the chemical basis for PI fluorescence in the pollen tube apical wall has not been established, we suspect that its positive charge allows the dye to interact with negative charges on pectin (i.e., carboxyl residues) in a manner similar to several other pectin dyes, such as ruthenium red (Ischebeck et al., 2008; Szumlanski and Nielsen, 2009), coriphosphine O (Weis et al., 1988), and cobalt and nickel (Varner and Taylor, 1989; Jauneau et al., 1997). That PI fluorescence and DIC thickness measurements provide nearly identical results strongly supports the conclusion that these two independent assays respond to the same feature. As shown in Table 1, thickness measurements on 10 lily pollen tubes reveal an advance over growth rate by a mean of –99°, while for PI fluorescence on 13 lily pollen tubes the mean advance is –97°. Equally compelling are the results in Figure 4C from the application of both methods on the same pollen tube; in this instance, DIC thickness precedes growth by –101°, while PI fluorescence precedes growth by –104°. Finally, we draw attention to the plasmolyzed lily pollen tube in Figure 4D, in which the DIC and PI fluorescence images virtually overlap in their portrayal of the highly thickened apical wall. The conclusion that these measurements indicate exocytosis derives strength from the observation in tobacco pollen tubes that the fluorescence signals from PI closely match those of PME-GFP, a probe that behaves as a direct marker for exocytosis. Furthermore, because PI fluorescence and wall thickness by DIC in lily pollen tubes yield the same result, we assert that all three methods effectively quantify the process of exocytosis.

A variety of factors, other than exocytosis, including the extracellular [Ca^{2+}], ionic strength, pH, and enzymatic activity can modify wall structure; to what extent might these affect the results we report? For example, following exocytosis, the pectin, which is initially 20 to 30% deesterified, becomes increasingly deesterified by PME, and cross-linked by Ca^{2+}, in a process that rigidifies and possibly compacts the wall (Willats et al., 2001; Bosch and Hepler, 2005). Additionally, the deesterification reaction yields methanol and protons; the former likely diffuses away quickly, while the latter could locally affect the cell wall pH and associated enzymes, such as PME itself (Moustacas et al., 1986; Li et al., 2002). These interactions will affect wall structure;

however, we do not think that they account for the observations we report. If PME were active immediately upon secretion, then Ca^{2+} influx should quickly follow. However, using a Ca^{2+} selective extracellular electrode, Holdaway-Clarke et al. (1997) found that ion influx follows growth by ~+130°, whereas PME secretion, as shown herein, leads growth by –128°. The phase difference may be due to the fact that PME is secreted as a full-length protein containing a proregion, which is presumed to be an endogenous inhibitor (Bosch et al., 2005). Following secretion, the proregion must be cleaved from the enzymatic domain; moreover, it may need to diffuse from the local region to permit full activity of the enzyme. These events may take some seconds and explain the phase separation between PME secretion and Ca^{2+} influx. In addition, the time interval means that these activities would be spatially displaced to the shoulders of the pollen tube apex and would not occur at the polar axis where the DIC, PI, and PME-GFP measurements have been made. From these considerations, we conclude that our data are not appreciably confounded by PME activity or Ca^{2+} binding. It is additionally pertinent that pollen tube growth occurs in a defined culture medium in which the [Ca^{2+}] as well as pH and other important ions, notably potassium, have been clamped at fixed levels. While there could be local changes of these factors in the wall itself, on balance, we think it is unlikely that they are of sufficient magnitude to account for the large-scale changes in cell wall properties we have observed. We conclude therefore that the changes observed in wall thickness and PI fluorescence result from changes in the appearance of new wall material along the polar axis and thus constitute a valid marker for exocytosis.

Exocytosis Has Been Studied in Other Pollen Tubes

Although the results presented herein are the first instance in which the temporal characteristics of exocytosis have been measured directly during oscillatory pollen tube growth, other studies have recorded the appearance of material at the cell surface (de Graaf et al., 2005; Lee et al., 2008) and attempted to infer the temporal properties. For example, Lee et al. (2008) noted that RabA4d, which brightly stained the inverted cone in tobacco pollen tubes, appeared to oscillate with a component close to the apex anticipating growth. Based on sequence homology, localization pattern, and sensitivity to Brefeldin A, this marker for membrane trafficking, which also labels apical membranes in *Arabidopsis thaliana* pollen tubes (Szumlanski and Nielsen, 2009), has been assumed to represent vesicles about to be secreted; however, no evidence of exocytosis has been provided. Lee et al. (2008) also observed that a receptor-like kinase fused to GFP stained the apical membrane. Fluorescence recovery after photobleaching analysis showed an active replacement of the signal at the apex with a half-time of 35 s. However, there were no data on whether the signal oscillated and what its relationship might be to growth. Instead, Lee et al. (2008) suggested that an oscillation in exocytosis will be in phase with the oscillation in the intracellular [Ca^{2+}] and thus closely follow growth. By contrast, the evidence presented herein indicates that exocytosis precedes the increase in growth rate by ~–100° in lily and is substantially out of phase with oscillations in the intracellular [Ca^{2+}] (see below).

Rather, more attention has been given to the location of exocytosis. Historically it has seemed obvious that vesicles move apically and aggregate in the inverted cone prior to secretion (Lancelle and Hepler, 1992; Cheung and Wu, 2008). However, the PME data in tobacco challenge this view by showing that the inverted cone stains much less brightly than the flanks surrounding the cone (Bosch et al., 2005; data herein). It is possible that material moves forward along the edge of the cell, being directed by the cortical actin fringe (Lovy-Wheeler et al., 2005), and deposits as an annulus outside of the polar axis (Bove et al., 2008; Zonia and Munnik, 2008), as has been shown for root hairs (Shaw et al., 2000; Dumais et al., 2004). This is an attractive idea, but more work is needed to establish its occurrence in pollen tubes.

The Amount of Wall Material Strongly Predicts the Growth Rate

An important conclusion emerging from this study is that the changes in wall material predict to a high degree the changes in growth rate. We propose, therefore, that the secretion and incorporation of new material into the wall holds the key to understanding the mechanism of wall relaxation and the acceleration in growth rate. The intercalation of new material into the cell wall matrix, or intussusception, may be sufficient to loosen and relax the wall, thus allowing extension (Ray, 1987). However, as emphasized by Ray (1987, 1992), the secretion (apposition) of material on to the inner wall surface does not reduce the wall tensile strength; material must be incorporated into the wall matrix in order for relaxation to occur.

Recent work from Proseus and Boyer (2005, 2006a, 2006b, 2006c) provides a mechanism for intercalation of secreted material that might apply to pollen tubes and, indeed, to plant cells in general. Using isolated primary cell walls of *Chara*, they introduced fluorescent dextrans of different sizes, which were then pressed against the inner surface of the wall by mineral oil from a pressure-controlled capillary (Proseus and Boyer, 2005, 2006a, 2006b). Pressures up to 0.5 MPa were sufficient to force dextrans from 4.4 to 70 kD, but not 580 kD, through the cell wall (Proseus and Boyer, 2005). They note that cells possess a thin periplasmic space between the plasma membrane and the inner surface of the wall, into which new wall material is initially secreted (Proseus and Boyer, 2006b). Because the new material lacks organization and load-bearing linkages, it will not provide structural resistance; therefore, turgor pressure will be exerted across the periplasmic space to the inner wall layer. The argument is made that turgor pressure within this layer will concentrate and mechanically drive large polymers into pores within the cell wall (Proseus and Boyer, 2005, 2006b). Of further interest, the addition of pectins, one of the components of the cell wall, allows these isolated *Chara* cells to achieve normal rates of elongation (Proseus and Boyer, 2006a, 2006c). Within this scenario it appears that the role of pectin is twofold: (1) insertion of new pectin molecules into the wall matrix would weaken existing linkages (intussusception), and (2) pectins already acted upon by PME would locally chelate Ca^{2+} and modulate the stiffening effect of this ion on cell wall structure (Boyer, 2009).

We suggest that these conditions apply to the tip of the pollen tube, and in Figure 8 we provide a working model. Exocytosis

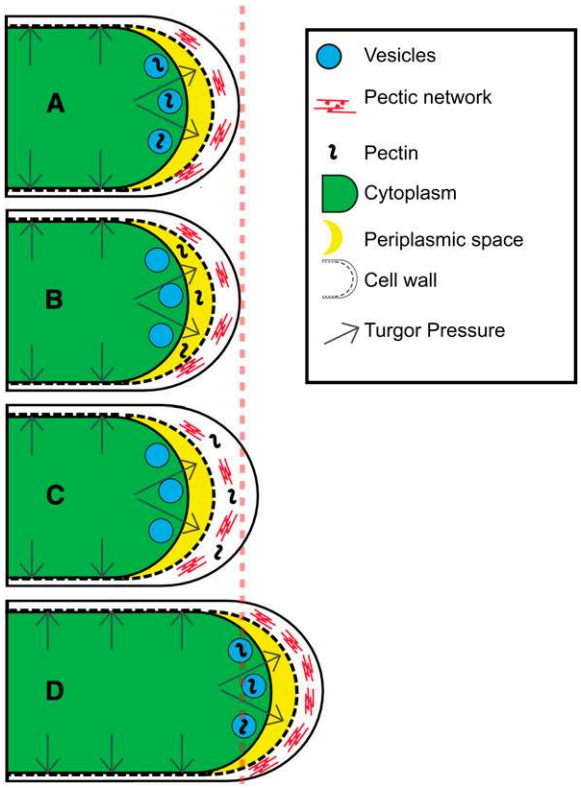

Figure 8. A Model That Portrays the Role of Exocytosis in Pollen Tube Growth.

In diagram A, the tube is in a slow growth phase. The cell wall is dominated by Ca^{2+} cross-linked pectic acids. Vesicles containing pectin, largely as esters, are poised for secretion. Diagram B depicts this same cell immediately after the vesicles have exocytosed their contents into the periplasmic space. In diagram C, we suggest that the turgor pressure, acting across the periplasmic space to the inner surface of the cell wall, forces these newly secreted pectins into the wall matrix and causes the apical wall to thicken. It is our view that turgor pressure, which is present at the same level in all panels, puts the cell wall under constant stress. Because the apical wall is less cross-linked with Ca^{2+} than the lateral walls, it is more readily deformed by the pressure, which may stretch existing bonds in ways that facilitate entry of new material. We suggest, in the transition from diagram C to diagram D, that the newly intercalated pectins weaken the existing cell wall bonds and allow turgor-dependent cell expansion. Finally, in diagram D, the newly introduced pectins have been deesterified by PME and their acidic residues cross-linked by Ca^{2+}. These activities stiffen the apical wall and return the cell to a slow-growing phase. However, vesicles containing pectin esters are again poised near the cell surface to begin a new round of exocytosis and growth.

delivers pectins, which are largely esterified, to the periplasmic space. Turgor pressure, which has been determined to be 0.1 to 0.4 MPa in lily (Benkert et al., 1997), forces these pectins into the wall matrix. In this model, it is our intention to indicate that turgor pressure is constant during growth, as experimentally measured by Benkert et al. (1997), and does not oscillate as proposed recently by Zonia and Munnik (2009). It seems plausible that the turgor pressure would stretch existing links in the apical wall and provide molecular openings for the insertion of the new material. Meanwhile, the nearby plasma membrane would prevent retrograde diffusion of the secreted pectins. Depending on the amount of pectin inserted into the wall, and the initial reduced cross-linking, either by Ca^{2+} or borate, cell wall extensibility increases and allows turgor-driven cell expansion. These considerations also help explain why turgor pressure per se is not correlated with the rate of growth in lily pollen tubes (Benkert et al., 1997). So long as turgor exists within a permissible range (i.e., 0.1 to 0.4 MPa for lily pollen tubes), newly secreted wall material will be forced into the wall, with the rate of expansion being dependent on the amount of wall material, as shown herein.

Over time, PME, which has also been secreted into the periplasm, progressively deesterifies the pectin, generating carboxyl groups that will be cross-linked by Ca^{2+} (Figure 8D). These reactions rigidify the apical cell wall and slow growth. A further consequence of pectin cross-linking by Ca^{2+} and borate will be a reduction in the pore size of the cell wall matrix (Baron-Epel et al., 1988; Fleischer et al., 1999). These changes in cell wall chemistry and structure, which will occur largely on the flanks of the apical dome, ensure that newly secreted material will only be inserted in the apical cell wall where cross-linking is lowest; taken together, these events contribute to the establishment and maintenance of cell polarity. In proposing the above model, we do not exclude a role for wall-loosening factors, such as expansin or degrading enzymes. However, applying Occam's razor, it is our view that specifically localized cell wall loosening and expansion in the pollen tube can be explained through the combined processes of intussusception, PME activity, and local Ca^{2+} regulation (Boyer, 2009).

Oscillation of the Intracellular [Ca^{2+}] Does Not Regulate Oscillatory Exocytosis

The analysis of the oscillatory exocytotic data produces at least one surprise and that stems from the lack of close phase relationship between the increase in secretion and the increase in the intracellular [Ca^{2+}]. Whereas in lily exocytosis leads growth by ~−100°, the increase in the intracellular [Ca^{2+}] follows growth by ~+10 to 40° (Messerli et al., 2000; Cárdenas et al., 2008). These two events are thus as much as 140° out of phase, and yet it is a paradigm in plant and animal cells (Battey et al., 1999), including pollen tubes (Roy et al., 1999; Camacho and Malhó, 2003), that Ca^{2+} stimulates secretion. How do we explain this apparent lack of correlation between Ca^{2+} and secretion? First, there is evidence in other plant systems that at least some secretion occurs independently of the [Ca^{2+}] (Homann and Tester, 1997). Second, we note that during normal growth, the [Ca^{2+}] is always high at the apical plasma membrane of the pollen tube. In lily pollen tubes, when the ion concentrations oscillate, they may drop only as low as 750 nM, but elevate to 3 μM (Pierson et al., 1996) or perhaps as high as 10 μM (Messerli et al., 2000). Even these values are almost certainly an underestimation since the domains immediately adjacent to the channels on the plasma membrane, where Ca^{2+} enters the cell and where secretion takes place, may well be considerably higher. From studies of maize (*Zea mays*) protoplasts, Sutter et al. (2000) have

shown that secretion is stimulated by a [Ca^{2+}], with half maximal saturation occurring at 900 nM and full saturation at 1500 nM. If the pollen tube secretory mechanism shows similar Ca^{2+} sensitivity, there may be a sufficient ion concentration even at the low point of the gradient to facilitate secretion, and raising the concentration further may not provide additional gain.

What are the regulators of oscillatory exocytosis? If changes in the [Ca^{2+}] do not regulate changes in exocytosis at the apex of the pollen tube, what then are the regulators? Recent studies have identified several anticipatory processes. First, F-actin amount and activity increases in the apical domain in anticipation of an increase in growth rate (Fu et al., 2001; Lovy-Wheeler et al., 2007; Cárdenas et al., 2008). Second, the alkaline band near the apex becomes more alkaline in anticipation of growth (~–80°) (Lovy-Wheeler et al., 2006), presumably due to a H^+-ATPase at the plasma membrane (Certal et al., 2008), whose activity oscillates. Third, Rops oscillate in activity, and recent work by Hwang et al. (2005) indicates that they lead growth (~–90°). Finally, NAD(P)H oscillates with $NAD(P)^+$, increasing in anticipation of an increase in the growth rate (~–80°) (Cárdenas et al., 2006). The oscillatory oxidation of NAD(P)H might indicate a similar oscillation in the synthesis of ATP, which could stimulate a variety of processes that enhance secretion. In brief, there are several leading events that could individually or in concert stimulate oscillatory growth.

In conclusion, our results show that exocytosis oscillates during pollen tube growth and leads the increase in growth rate. Statistical analyses of these data reveal a high degree of correlation between the anticipatory exocytotic events and the subsequent rate and extent of growth. We interpret these results as support for the idea that exocytosis and the amount of wall material are critical components of the processes that determine the growth rate. We suggest that secretion adds pectins to the periplasmic space and that turgor pressure forces these molecules into the wall matrix. This process of intercalation of new wall components, together with local Ca^{2+} chelation, relaxes the cell wall and allows turgor-dependent tube extension. Exocytosis thus emerges as a potential initiator of growth.

METHODS

Pollen Culture

Pollen grains from *Lilium longiflorum* and *Lilium formosanum* were cultured in lily pollen growth medium composed of 15 mM MES, 1.6 mM H_3BO_3, 1 mM KCl, 0.1 to 0.2 mM $CaCl_2$, and 7% (w/v) sucrose at pH 5.9. Although the original observations of oscillations in apical cell wall thickness were made in *L. longiflorum*, we soon discovered that the same changes occurred in *L. formosanum*. As a consequence, both species were used interchangeably; *Nicotiana tabacum* pollen was cultured in tobacco pollen growth medium (TPGM) composed of 20 mM MES, 0.07% (w/v) $Ca(NO_3)_2 \cdot 4\,H_2O$, 0.02% (w/v) $MgSO_4$, 0.01% (w/v) H_3BO_3, 0.01% (w/v) KNO_3, 2% (w/v) sucrose, and 15% (w/v) PEG 3350 at pH 6.0. Pollen grains were germinated and grown in their respective medium on a rotor at room temperature for ~1 h. Actively growing pollen tubes were immobilized with low melting point agarose type VII (Sigma-Aldrich), at a final concentration of 0.7% (w/v) diluted in the respective growth medium, plated in an open glass slide chamber, and overlaid with growth medium. Pollen tubes were allowed to recover for 1 h in a moist chamber before they were subjected to experimentation and observation. While most pollen tubes show robust growth rate oscillation, not all show readily measurable changes in apical cell wall thickness because the dimensions are close to the limit of resolution of our optical system. Through trial and error we found that a slightly higher, but nonplasmolyzing, concentration of sucrose (9.5%) often yielded a greater number of cells exhibiting resolvable changes in apical wall thickness. These culture conditions, which had no effect on growth rate or any other vital signs, were preferentially used in the studies where changes in apical cell wall thickness were being measured using DIC optics.

Staining of Pollen Tubes

PI (Molecular Probes) was used as a cell wall marker (Fiers et al., 2005). Staining of pollen tubes was achieved by addition of PGM containing 30 or 60 μM PI to pollen tubes, which were actively growing after immobilization in low gelling temperature agarose (Sigma-Aldrich type VII). Images were taken while pollen tubes were submerged in the dye, at least 15 min after the dye was added.

PME Secretion

The tobacco pollen-specific construct Lat52-NtPPME1-GFP, which had previously been designed for the localization of *N. tabacum* PPME1 (Bosch et al., 2005), was employed to show the dynamics of PME secretion. Two to three micrograms of Lat52 PME-GFP plasmid DNA was coated onto 3 mg of tungsten particles according to the manufacturer's procedure and then divided and dried on two macrocarriers (Bio-Rad Laboratories) for bombardment. Approximately 10 mg of pollen was hydrated in 1 mL of TPGM for 5 min and evenly spread on a 25-mm MF-Millipore membrane, positioned at the center of a moist Whatman filter paper in a 60 × 15-mm Petri dish. For these studies, the TPGM was modified slightly; the PEG was removed and the sucrose increased from 2 to 7%. Microprojectile bombardment was performed using a Bio-Rad helium-driven particle accelerator, PDS-1000/He Biolistic system (Bio-Rad) with 1100-p.s.i. rupture discs. Each sample of pollen was bombarded twice, each time with one of the two macrocarriers with plasmid DNA. Bombarded pollen was transferred to an Eppendorf tube with TPGM, allowed to germinate, plated as above, and kept in a moist chamber for 3 h before images were taken.

Microscopy and Image Acquisition

For visualization of wall thickness, observations were performed with Nomarski DIC on a Nikon Eclipse TE300 inverted microscope, equipped either with a ×40 oil immersion lens (NA = 1.3) or a ×60 oil immersion lens (NA = 1.4). Transmitted light was generated by a low-voltage halogen lamp. For the highest resolution, we also included an oil immersion condenser (NA = 1.4). A filter wheel (Lambda 10; Sutter Instruments), positioned immediately before the CCD camera, was programmed to insert an analyzer filter, in order to permit rapid switching between DIC and fluorescence imaging (see PI fluorescence imaging below). Images were acquired with a cooled CCD camera (Quantix Cool Snap HQ; Photometrics), driven by MetaMorph/MetaFluor software (Molecular Devices). The exposure times were ~50 ms. The time-series intervals between successive images were 1 to 3 s for lily and 10 s for tobacco.

Fluorescence imaging was performed with a Nikon epi-wide-field fluorescence microscope or with different confocal microscopes (Zeiss 510-Meta or Nikon D-Eclipse C1). For a variety of reasons, stemming mainly from a better choice of excitation wavelengths and speed of image acquisition, the PI fluorescence data were largely obtained by wide-field fluorescence. However, it should be noted that we made close comparisons of the PI signal using both microscope systems and concluded that the improved resolution in the *z* axis, afforded by the confocal

microscope, did not provide different or clearer results. Cells stained with PI were excited at 535 nm, and emission was collected at 615 nm. Fluorescence excitation light came from a 175-W ozone-free xenon lamp in a DG-4 ultra-high-speed wavelength switching system (Sutter Instruments).

Confocal images obtained on the Zeiss 510 Meta laser scanning microscope system were acquired using a plan-apo-chromat ×63 oil immersion lens (NA = 1.4); with the Nikon D-Eclipse C1, we used a ×60 water immersion lens (NA = 1.2). Cells expressing GFP-tagged proteins were also examined by confocal microscopy. Images were acquired using an excitation at 488 nm (argon laser) and emission at 505 nm; a time-series interval of 10 s was used for tobacco.

Determination of Wall Thickness, Fluorescence, and Growth Rate

Using DIC optics, we have been able to consistently visualize a region at the tip of growing lily pollen tubes, outside the cell contents of the pollen tube and distinct from the surrounding medium. Because DIC creates contrast from gradients in refractive index, we interpret the boundaries of this region to be determined by the transitions in optical properties between cytoplasm and cell wall and between cell wall and growth medium. While we know from electron microscopy that these transitions are in actuality quite sharp, even at the Nyquist limit in DIC optics the cell wall edges appear as Gaussian distributions of intensity (i.e., fringes) encoded in several pixels across the region. We have developed an interpolation method that allows us to model the patterns in contrast along a transect normal to the pollen tube edge as the sum of a pair of Gaussian distributions, thereby inferring the distance between the cytoplasm/cell wall and cell wall/medium transitions (i.e., wall thickness). A detailed treatment and R scripts are provided in Supplemental Data Sets 1 and 2 online.

In practice, we use an interactive R script to manipulate six parameters, three for each fringe (location, height, and variance) until the predicted intensity distribution matches the data as closely as possible. Typically, distance between peaks varies smoothly and has the greatest effect upon the fringe pattern, while peak width and intensity vary randomly within small ranges, thus increasing our confidence that we are extracting valid thickness measurements.

Growth rate was measured as the difference in location of the pollen tube tip in the image frame in two successive frames divided by the time between each frame capture. In PI experiments, the tube tip was determined using the profile in PI fluorescence, which always peaked at the leading edge of the tube. In the PME-GFP experiments, we used the Object Tracking protocol in MetaMorph (Molecular Devices) to trace the location and motion of the tube tip. PME-GFP and PI images were analyzed with a custom R script (available upon request) that determined the maximum average fluorescence intensity at the tip of the growing cell along a stripe 7 pixels wide (1.4 μm) down the midline of the cell in each image in a time-lapse sequence.

Statistical Analysis of Thickness, PI Staining, and Growth Rate

Cross-correlations between growth rate with wall thickness and PI fluorescence and between PI fluorescence and wall thickness were performed with a custom R script (see Supplemental Data Set 2 online) as previously described (Holdaway-Clarke et al., 1997; Cárdenas et al., 2006; Lovy-Wheeler et al., 2006). Detailed results and R code are available upon request. To test the ability of wall thickness or PI staining to predict growth rate, we first created six data sets containing growth rates and tip thicknesses or PI fluorescence from individual pollen tubes using the methods described above. For each data set, we correlated growth rates at each time point with tip thickness at time offsets from −21 to +21 s in intervals of 3 s. These data sets consisted of a sequence of frames collected at 3-s intervals, so the selected offsets corresponded to shifts of from one to seven frames before or after the time point in question. Once the offsets with the most predictive value were determined, we used a GLM to predict growth rate at a particular time point from a set of thickness values at specific time offsets from the time point in question. Correlation analysis of thickness and growth rate showed that offsets of −6, −3, 0, 3, and 6 s (frames −2, −1, 0, 1, and 2) had little predictive value and so were not used in the GLM analysis. Correlation of PI staining and growth rate was performed using the same technique for generating a matrix of independent variables using time offsets that were then analyzed using the same custom GLM program or the multiple linear regression function, lm, in R (Maindonald and Braun, 2007). Detailed procedures and R scripts are provided in Supplemental Data Sets 1 and 2 online.

Accession Number

Sequence data of *N. tabacum* PPME1 have been deposited with the GenBank/NCBI databases under accession number AY772945.

Supplemental Data

The following materials are available in the online version of this article.

Supplemental Figure 1. Use of Plasmolysis to Show That Full-Length PME-GFP Is Secreted.

Supplemental Data Set 1. Gaussian Fitting, GAM, and GLM, and R Scripts.

Supplemental Data Set 2. Text File of R Scripts.

Supplemental Movie 1. DIC Image of Lily Pollen Tube Showing Oscillating Wall Thickness.

Supplemental Movie 2. PI Staining of Lily Pollen Tube.

Supplemental Movie 3. PI Staining of Tobacco Pollen Tube.

Supplemental Movie 4. Tobacco Pollen Tube Expressing PME-GFP.

Supplemental Movie Legends.

ACKNOWLEDGMENTS

We thank our colleagues, notably Tobias Baskin and Magdalena Bezanilla, and members of their respective laboratory groups, for many helpful discussions during the course of this study. This project was supported by National Science Foundation Grant MCB-0516852 to P.K.H.

Received June 11, 2009; revised September 28, 2009; accepted October 14, 2009; published October 27, 2009.

REFERENCES

Baron-Epel, O., Hernandez, D., Jiang, L.W., Meiners, S., and Schindler, M. (1988). Dynamic continuity of cytoplasmic and membrane compartments between plant cells. J. Cell Biol. **106:** 715–721.

Battey, N.H., James, N.C., Greenland, A.J., and Brownlee, C. (1999). Exocytosis and endocytosis. Plant Cell **11:** 643–660.

Benkert, R., Obermeyer, G., and Bentrup, F.W. (1997). The turgor pressure of growing lily pollen tubes. Protoplasma **198:** 1–8.

Bosch, M., Cheung, A.Y., and Hepler, P.K. (2005). Pectin methylesterase, a regulator of pollen tube growth. Plant Physiol. **138:** 1334–1346.

Bosch, M., and Hepler, P.K. (2005). Pectin methylesterases and pectin dynamics in pollen tubes. Plant Cell **17:** 3219–3226.

Bove, J., Vaillancourt, B., Kroeger, J., Hepler, P.K., Wiseman, P.W., and Geitmann, A. (2008). Magnitude and direction of vesicle dynamics in growng pollen tubes using spatiotemporal image correlation spectroscopy (STICS). Plant Physiol. **147:** 1646–1658.

Boyer, J.S. (2009). Cell wall biosynthesis and the molecular mechanism of plant enlargement. Funct. Plant Biol. **36:** 383–394.

Brewbaker, J.L., and Kwack, B.H. (1963). The essential role of calcium ion in pollen germination and pollen tube growth. Am. J. Bot. **50:** 859–865.

Camacho, L., and Malhó, R. (2003). Endo/exocytosis in the pollen tube apex is differentially regulated by Ca^{2+} and GTPases. J. Exp. Bot. **54:** 83–92.

Campanoni, P., and Blatt, M.R. (2007). Membrane trafficking and polar growth in root hairs and pollen tubes. J. Exp. Bot. **58:** 65–74.

Cárdenas, L., Lovy-Wheeler, A., Kunkel, J.G., and Hepler, P.K. (2008). Pollen tube growth oscillations and intracellular calcium levels are reversibly modulated by actin polymerization. Plant Physiol. **146:** 1611–1621.

Cárdenas, L., McKenna, S.T., Kunkel, J.G., and Hepler, P.K. (2006). NAD(P)H oscillates in pollen tubes and is correlated with tip growth. Plant Physiol. **142:** 1460–1468.

Catoire, L., Pierron, M., Morvan, C., du Penhoat, C.H., and Goldberg, R. (1998). Investigation of the action patterns of pectinmethylesterase isoforms through kinetic analyses and NMR spectroscopy. Implications in cell wall expansion. J. Biol. Chem. **273:** 33150–33156.

Certal, A.C., Almeida, R.B., Carvalho, L.M., Wong, E., Moreno, N., Michard, E., Carneiro, J., Rodriguéz-Léon, J., Wu, H.M., Cheung, A.Y., and Feijó, J.A. (2008). Exclusion of a proton ATPase from the apical membrane is associated with cell polarity and tip growth in *Nicotiana tabacum* pollen tubes. Plant Cell **20:** 614–634.

Chebli, Y., and Geitmann, A. (2007). Mechanical principles governing pollen tube growth. Floricul. Ornamen. Biotech. **1:** 232–245.

Cheung, A.Y., and Wu, H.M. (2008). Structural and signaling networks for the polar cell growth machinery in pollen tubes. Annu. Rev. Plant Biol. **59:** 547–572.

Cole, R.A., and Fowler, J.E. (2006). Polarized growth: Maintaining focus on the tip. Curr. Opin. Plant Biol. **9:** 579–588.

Cryer, J.D., and Chan, K.-S. (2008). Time Series Analysis with Applications in R, 2nd ed. (New York: Springer).

de Graaf, B.H., Cheung, A.Y., Andreyeva, T., Levasseur, K., Kieliszewski, M., and Wu, H.M. (2005). Rab11 GTPase-regulated membrane trafficking in crucial for tip-focused pollen tube growth in tobacco. Plant Cell **17:** 2564–2579.

Dumais, J., Long, S.R., and Shaw, S.L. (2004). The mechanics of surface expansion anisotropy in *Medicago truncatula* root hairs. Plant Physiol. **136:** 3266–3275.

Estevez, J.M., Leonardi, P.I., and Alberghina, J.S. (2008). Cell wall carbohydrate epitopes in the green alga *Oedogonium bharuchae* F. Minor (Oedogoniales, Chlorophyta). J. Phycol. **44:** 1257–1268.

Feijó, J.A., Sainhas, J., Holdaway-Clarke, T., Cordeiro, M.S., Kunkel, J.G., and Hepler, P.K. (2001). Cellular oscillations and the regulation of growth: The pollen tube paradigm. Bioessays **23:** 86–94.

Fiers, M., Golemiec, E., Xu, J., van der Geest, L., Heidstra, R., Stiekema, W., and Liu, C.M. (2005). The 14-amino acid CLV3, CLE19, and CLE40 peptides trigger consumption of the root meristem in *Arabidopsis* through a CLAVATA2-dependent pathway. Plant Cell **17:** 2542–2553.

Fleischer, A., O'Neill, M.A., and Ehwald, R. (1999). The pore size of non-graminaceous plant cell walls is rapidly decreased by borate ester cross-linking of the pectic polysaccharide rhamnogalacturonan II. Plant Physiol. **121:** 829–838.

Fu, Y., Wu, G., and Yang, Z. (2001). Rop GTPase-dependent dynamics of tip-localized f-actin controls tip growth in pollen tubes. J. Cell Biol. **152:** 1019–1032.

Geitmann, A., Li, Y.Q., and Cresti, M. (1996). The role of the cytoskeleton and dictyosome activity in the pulsatory growth of *Nicotiana tabacum* and *Petunia hybrida* pollen tubes. Bot. Acta **109:** 102–109.

Heslop-Harrison, J. (1987). Pollen germination and pollen-tube growth. Int. Rev. Cytol. **107:** 1–78.

Holdaway-Clarke, T.L., Feijó, J.A., Hackett, G.R., Kunkel, J.G., and Hepler, P.K. (1997). Pollen tube growth and the intracellular cytostolic calcium gradient oscillate in phase while extracellular calcium influx is delayed. Plant Cell **9:** 1999–2010.

Holdaway-Clarke, T.L., and Hepler, P.K. (2003). Control of pollen tube growth: role of ion gradients and fluxes. New Phytol. **159:** 539–563.

Homann, U., and Tester, M. (1997). Ca^{2+}-independent and Ca^{2+}/GTP-binding protein-controlled exocytosis in a plant cell. Proc. Natl. Acad. Sci. USA **94:** 6565–6570.

Hwang, J.U., Gu, Y., Lee, Y.J., and Yang, Z. (2005). Oscillatory ROP GTPase activation leads the oscillatory polarized growth of pollen tubes. Mol. Biol. Cell **16:** 5385–5399.

Ischebeck, T., Stenzel, I., and Heilmann, I. (2008). Type B phosphatidylinositol-4-phosphate 5-kinases mediate *Arabidopsis* and *Nicotiana tabacum* pollen tube growth by regulating apical pectin secretion. Plant Cell **20:** 3312–3330.

Ishii, T., Matsunaga, T., Pellerin, P., O'Neill, M.A., Darvill, A., and Albersheim, P. (1999). The plant cell wall polysaccharide rhamnogalacturonan II self-assembles into a covalently cross-linked dimer. J. Biol. Chem. **274:** 13098–13104.

Jauneau, A., Quentin, M., and Driouich, A. (1997). Micro-heterogeneity of pectins and calcium distribution in the epidermal and cortical parenchyma cell walls of flax hypocotyl. Protoplasma **198:** 9–19.

Ketelaar, T., Galway, M.E., Mulder, B.M., and Emons, A.M.C. (2008). Rates of exocytosis and endocytosis in *Arabidopsis* root hairs and pollen tubes. J. Microsc. **231:** 265–273.

Krichevsky, A., Kozlovsky, S.V., Tian, G.W., Chen, M.H., Zaltsman, A., and Citovsky, V. (2007). How pollen tubes grow. Dev. Biol. **303:** 405–420.

Lancelle, S.A., and Hepler, P.K. (1988). Cytochalasin-induced ultrastructural alterations in *Nicotiana* pollen tubes. Protoplasma (suppl. 2): 65–75.

Lancelle, S.A., and Hepler, P.K. (1992). Ultrastructure of freeze-substituted pollen tubes of *Lilium longiflorum.* Protoplasma **167:** 215–230.

Lee, Y.J., Szumlanski, A., Nielsen, E., and Yang, Z. (2008). Rho-GTPase-dependent filamentous actin dynamics coordinate vesicle targeting and exocytosis during tip growth. J. Cell Biol. **181:** 1155–1168.

Li, Y.Q., Faleri, C., Geitmann, A., Zhang, H.Q., and Cresti, M. (1995). Immunogold localization of arabinogalactan proteins, unesterified and esterified pectins in pollen grains and pollen tubes of *Nicotiana tabacum* L. Protoplasma **189:** 26–36.

Li, Y.Q., Mareck, A., Faleri, C., Moscatelli, A., Liu, Q., and Cresti, M. (2002). Detection and localization of pectin methylesterase isoforms in pollen tubes of *Nicotiana tabacum* L. Planta **214:** 734–740.

Lovy-Wheeler, A., Cárdenas, L., Kunkel, J.G., and Hepler, P.K. (2007). Differential organelle movement on the actin cytoskeleton in lily pollen tubes. Cell Motil. Cytoskeleton **64:** 217–232.

Lovy-Wheeler, A., Kunkel, J.G., Allwood, E.G., Hussey, P.J., and Hepler, P.K. (2006). Oscillatory increases in alkalinity anticipate growth and may regulate actin dynamics in pollen tubes of lily. Plant Cell **18:** 2182–2193.

Lovy-Wheeler, A., Wilsen, K.L., Baskin, T.I., and Hepler, P.K. (2005). Enhanced fixation reveals the apical cortical actin fringe of actin

microfilaments as a consistent feature of the pollen tube. Planta **221:** 95–104.

Maindonald, J., and Braun, J. (2007). Data Analysis and Graphics Using R: An Example-Based Approach, 2nd ed. (Cambridge, UK: Cambridge University Press).

Malhó, R., Read, N.D., Pais, M.S., and Trewavas, A.J. (1994). Role of cytosolic free calcium in the reorientation of pollen tube growth. Plant J. **5:** 331–341.

Mascarenhas, J.P. (1993). Molecular mechanisms of pollen tube growth and differentiation. Plant Cell **5:** 1303–1314.

Messerli, M.A., Creton, R., Jaffe, L.F., and Robinson, K.R. (2000). Periodic increases in elongation rate precede increases in cytosolic Ca^{2+} during pollen tube growth. Dev. Biol. **222:** 84–98.

Miller, D.D., Callaham, D.A., Gross, D.J., and Hepler, P.K. (1992). Free Ca^{2+} gradient in growing pollen tubes of *Lilium.* J. Cell Sci. **101:** 7–12.

Moreno, N., Colaco, R., and Feijó, J.A. (2007). The pollen tube oscillator: Integrating biophysics and biochemistry into cellular growth and morphogenesis. In Rhythms in Plants: Phenomenology, Mechanisms, and Adaptive Significance, S. Mancuso and S. Shabala, eds (Berlin: Springer-Verlag), pp. 39–62.

Moscatelli, A., Ciampolini, F., Rodighiero, S., Onelli, E., Cresti, M., Santo, N., and Idilli, A. (2007). Distinct endocytic pathways identified in tobacco pollen tubes using charged nanogold. J. Cell Sci. **120:** 3804–3819.

Moustacas, A.M., Nari, J., Diamantidis, G., Noat, G., Crasnier, M., Borel, M., and Ricard, J. (1986). Electrostatic effects and the dynamics of enzyme reactions at the surface of plant cells. 2. The role of pectin methyl esterase in the modulation of electrostatic effects in soybean cell walls. Eur. J. Biochem. **155:** 191–197.

Nebenführ, A., and Staehelin, L.A. (2001). Mobile factories: Golgi dynamics in plant cells. Trends Plant Sci. **6:** 160–167.

O'Neill, M.A., Albersheim, P., and Darvill, A. (1990). The pectic polysaccharides of primary cell walls. In Methods in Plant Biochemistry, Carbohydrates, P.M. Dey and J.B. Harborne, eds (London: Academic Press), pp. 415–441.

O'Neill, M.A., Eberhard, S., Albersheim, P., and Darvill, A.G. (2001). Requirement of borate cross-linking of cell wall rhamnogalacturonan II for Arabidopsis growth. Science **294:** 846–849.

O'Neill, M.A., Ishii, T., Albersheim, P., and Darvill, A.G. (2004). Rhamnogalacturonan II: Structure and function of a borate cross-linked cell wall pectic polysaccharide. Annu. Rev. Plant Biol. **55:** 109–139.

Parton, R.M., Fischer-Parton, S., Watahiki, M.K., and Trewavas, A.J. (2001). Dynamics of the apical vesicle accumulation and the rate of growth are related in individual pollen tubes. J. Cell Sci. **114:** 2685–2695.

Picton, J.M., and Steer, M.W. (1983). Membrane recycling and the control of secretory activity in pollen tubes. J. Cell Sci. **63:** 303–310.

Pierson, E.S., Li, Y.Q., Zhang, G.Q., Willemse, M.T.M., Linskens, H. F., and Cresti, M. (1995). Pulsatory growth of pollen tubes: Investigation of a possible relationship with the periodic distribution of cell wall components. Acta. Bot. Neerl. **44:** 121–128.

Pierson, E.S., Miller, D.D., Callaham, D.A., Shipley, A.M., Rivers, B. A., Cresti, M., and Hepler, P.K. (1994). Pollen tube growth is coupled to the extracellular calcium ion flux and the intracellular calcium gradient: Effect of BAPTA-Type buffers and hypertonic media. Plant Cell **6:** 1815–1828.

Pierson, E.S., Miller, D.D., Callaham, D.A., van Aken, J., Hackett, G., and Hepler, P.K. (1996). Tip-localized calcium entry fluctuates during pollen tube growth. Dev. Biol. **174:** 160–173.

Plyushch, T.A., Willemse, M.T.M., Franssen-Verheijen, M.A.W., and Reinders, M.C. (1995). Structural aspects of in vitro pollen tube growth and micropylar penetration in *Gasteria verrucosa* (Mill.) H. Duval and *Lilium longiflorum* thumb. Protoplasma **187:** 13–21.

Proseus, T.E., and Boyer, J.S. (2005). Turgor pressure moves polysaccharides into growing cell walls of *Chara corallina.* Ann. Bot. (Lond.) **95:** 967–979.

Proseus, T.E., and Boyer, J.S. (2006a). Identifying cytoplasmic input to the cell wall of growing *Chara corallina.* J. Exp. Bot. **57:** 3231–3242.

Proseus, T.E., and Boyer, J.S. (2006b). Periplasm turgor pressure controls wall deposition and assembly in growing *Chara corallina* cells. Ann. Bot. (Lond.) **98:** 93–105.

Proseus, T.E., and Boyer, J.S. (2006c). Calcium pectate chemistry controls growth rate of *Chara corallina.* J. Exp. Bot. **57:** 3989–4002.

Rao, C.R. (1965). Linear Statistical Inference and Its Applications. (New York: John Wiley & Sons).

Rathore, K.S., Cork, R.J., and Robinson, K.R. (1991). A cytoplasmic gradient of Ca^{2+} is correlated with the growth of lily pollen tubes. Dev. Biol. **148:** 612–619.

Ray, P.M. (1987). Principles of plant cell expansion. In Physiology of Cell Expansion during Plant Growth, D.J. Cosgrove and D.P. Knievel, eds (Washington, DC: American Society of Plant Physiologists), pp. 1–17.

Ray, P.M. (1992). Mechanisms of wall loosening for cell growth. Curr. Top. Plant Biochem. Physiol. **11:** 18–41.

Roy, S.J., Holdaway-Clarke, T.L., Hackett, G.R., Kunkel, J.G., Lord, E.M., and Hepler, P.K. (1999). Uncoupling secretion and tip growth in lily pollen tubes: evidence for the role of calcium in exocytosis. Plant J. **19:** 379–386.

Shaw, S.L., Dumais, J., and Long, S.R. (2000). Cell surface expansion in polarly growing root hairs of *Medicago truncatula.* Plant Physiol. **124:** 959–970.

Shumway, R.H., and Stoffer, D.S. 2006. Time Series Analysis and Its Applications with R Examples, 2nd ed. (New York: Springer).

Staehelin, L.A., and Moore, I. (1995). The plant Golgi apparatus: Structure, functional organization and trafficking mechanisms. Annu. Rev. Plant Physiol. Plant Mol. Biol. **46:** 261–288.

Steer, M.W., and Steer, J.M. (1989). Pollen tube tip growth. New Phytol. **111:** 323–358.

Sterling, J.D., Quigley, H.F., Orellana, A., and Mohnen, D. (2001). The catalytic site of the pectin biosynthetic enzyme alpha-1,4- galacturonosyltransferase is located in the lumen of the Golgi. Plant Physiol. **127:** 360–371.

Sutter, J.U., Homann, U., and Thiel, G. (2000). Ca^{2+}-stimulated exocytosis in maize coleoptile cells. Plant Cell **12:** 1127–1136.

Szumlanski, A.L., and Nielsen, E. (2009). The Rab GTPase RabA4d regulates pollen tube tip growth in *Arabidopsis thaliana.* Plant Cell **21:** 526–544.

Tian, G.W., Chen, M.H., Zaltsman, A., and Citovsky, V. (2006). Pollen-specific pectin methylesterase involved in pollen tube growth. Dev. Biol. **294:** 83–91.

Varner, J.E., and Taylor, R. (1989). New ways to look at the architecture of plant cell walls: Localization of polygalacturonate blocks in plant tissues. Plant Physiol. **91:** 31–33.

Weis, K.G., Polito, V.S., and Labavitch, J.M. (1988). Microfluorometry of pectic materials in the dehiscence zone of almond (*Prunus dulcis* [Mill.] DA Webb) fruits. J. Histochem. Cytochem. **36:** 1037–1041.

Willats, W.G.T., McCartney, L., Mackie, W., and Knox, J.P. (2001). Pectin: Cell biology and prospects for functional analysis. Plant Mol. Biol. **47:** 9–27.

Zonia, L., and Munnik, T. (2008). Vesicle trafficking dynamics and visualization of zones of exocytosis and endocytosis in tobacco pollen tubes. J. Exp. Bot. **59:** 861–873.

Zonia, L., and Munnik, T. (2009). Uncovering hidden treasures in pollen tube growth mechanics. Trends Plant Sci. **14:** 318–327.